Available online at www.sciencedirect.com
SCIENCE DIRECT®
ELSEVIER
Earth and Planetary Science Letters 212 (2003) 291–306
EPSL
www.elsevier.com/locate/epsl

Mg/Ca variation in planktonic foraminifera tests: implications for reconstructing palaeo-seawater temperature and habitat migration

Stephen Eggins [a,*], Patrick De Deckker [b], John Marshall [a]

[a] *Research School of Earth Sciences, The Australian National University, Canberra, ACT 0200, Australia*
[b] *Department of Geology, The Australian National University, Canberra, ACT 0200, Australia*

Received 5 December 2002; received in revised form 14 May 2003; accepted 15 May 2003

Abstract

The nature of compositional variability within the tiny calcitic shells (tests) that are precipitated by planktonic foraminifera has been investigated using laser ablation inductively coupled plasma mass spectrometry (LA-ICP-MS). Systematic large and correlated variation of Mg/Ca, Mn/Ca, Ba/Ca and Zn/Ca but relatively uniform Sr/Ca are observed through the test walls of analysed species (*Globigerinoides sacculifer*, *Globigerinoides ruber*, *Neogloboquadrina pachyderma* and *Neogloboquadrina dutertrei*). Distinct chamber and chamber-wall layer compositions can be resolved within individual tests, and Mg/Ca compositional differences observed in sequentially precipitated test components of the different species analysed are consistent with seawater temperature changes occurring with habitat migration during their adult life-cycle stages. Estimated test calcification temperatures are in keeping with available seawater temperature constraints, indicating the potential for accurate seawater temperature reconstruction using LA-ICP-MS. Mg-rich ($<$1–6 mol% Mg) surface veneers that are also enriched in Mn, Ba, and Zn have been found on all species and all fossil tests, as well as on live-sampled tests of *G. ruber*, with the latter suggesting a possible biogenic origin. These Mg-rich surfaces bias bulk test compositions toward higher Mg/Ca values by between 5 and 35%.

Keywords: Mg/Ca seawater thermometry; trace elements; laser ablation ICP-MS; planktonic foraminifera; palaeoceanography

1. Introduction

The incorporation of Mg into the tiny calcitic shells (tests) that are secreted by planktonic foraminifera is extraordinarily sensitive to calcification temperature and is the basis of a new and rapidly emerging tool for reconstructing palaeo-seawater temperature. Large exponential increases in shell Mg/Ca ratio, of the order of $10 \pm 1\%$ per °C, have been documented under both controlled laboratory conditions and in modern shell material recovered from seafloor sediments [1–4]. These relationships underpin a range of seawater thermometer calibrations that may be applied to a small but expanding number of planktonic foraminifera species [1–7]. Given the widespread dis-

* Corresponding author.
E-mail address: stephen.eggins@anu.edu.au (S. Eggins).

0012-821X/03/$ – see front matter © 2003 Elsevier Science B.V. All rights reserved.
doi:10.1016/S0012-821X(03)00283-8

tribution and abundance of fossil foraminifera tests in deep-sea sediments, these thermometers are proving invaluable for reconstructing long and detailed records of temperature change in the oceans [4–7]. This complements the use of several other trace elements and stable isotopes in foraminiferal calcite, most notably $\delta^{18}O$ but also $\delta^{13}C$, Cd, Ba, Zn and Sr, which are established proxies for past seawater temperature, composition, nutrient levels, and productivity [8,9]. Moreover, by combining Mg/Ca thermometry with $\delta^{18}O$ measurements on the same shell material, palaeo-seawater $\delta^{18}O$ can be isolated from the temperature-dependent fractionation of $\delta^{18}O$ that occurs during shell precipitation [7,10,11], and palaeo-salinity (and seawater density) can be estimated from relationships between seawater $\delta^{18}O$, temperature and salinity [12]. The constraint of seawater temperature and salinity from the Mg/Ca and $\delta^{18}O$ compositions of foraminiferal calcite presents the possibility of reconstructing past changes in glacial ice volume, local precipitation/evaporation, and water mass density. Establishing spatial and temporal changes in these variables is fundamental to evaluating linked palaeocean and palaeo-climate events, and forecasting the nature and rate of future climate change [13,14].

In this study we investigate the distribution of Mg/Ca and several other trace elements within the tests of a small number of planktonic species that are commonly employed for palaeocean reconstruction. This has been driven by the need to understand those factors that influence the incorporation of Mg into foraminiferal calcite, the significance of bulk test Mg/Ca compositions, and the reliability and accuracy of Mg/Ca thermometry as currently applied to different planktonic foraminifera species. The feasibility of applying laser ablation inductively coupled plasma mass spectrometry (LA-ICP-MS) to analyse Mg/Ca and other trace elements in planktonic foraminifera is also demonstrated.

2. Background

Mg/Ca in the tests of many planktonic species has been shown to vary as an exponential function of calcification temperature (i.e. $Mg/Ca = A\exp^{BT}$) [1,2,4]. The exponential temperature dependence (B) appears to be similar for all planktonic species and is within the range 0.10 ± 0.01. However, calibrations for different species are often characterised by significantly different values for the pre-exponential constant (A). Moreover, where more than one Mg/Ca thermometer calibration has been determined for the same species (e.g. *Globigerinoides sacculifer* or *Globigerinoides ruber*), significant disagreement is often found in derived seawater temperature estimates that cannot be accounted for by typically quoted calibration uncertainties (i.e. ± 0.5–1.5°C [7,15,16]). It has become apparent that differences between these same species calibrations reflect, in part, the variable preservation of deep-sea core material due to the lowering of bulk test Mg/Ca compositions by seafloor dissolution [15,16,17]. This process preferentially dissolves and removes more Mg-rich test compositions with decreasing carbonate ion activity and increasing depth in the oceans [17]. A method of correcting for these changes in bulk test Mg/Ca composition, based on the reduced weight of dissolution-affected tests, has been proposed recently for *G. ruber* and *G. sacculifer* [18]. It should also be noted that some calibrations are referenced to sea-surface temperature (SST) and others to calcification temperature, which can differ significantly for species other than those that calcify near the surface (e.g. *G. ruber*).

Mg/Ca thermometry is conventionally applied by analysis of between five and 50 whole fossil tests of the same species. Mg/Ca ratios can be measured using this approach to better than 1% reproducibility with modern instrumental techniques [19,20], which suggests the possibility of constraining palaeo-seawater temperatures to within a few tenths of a °C. However, in practice, achieving this degree of accuracy and precision is compromised by: (1) compositional variation within a population of tests due to the calcification of individual foraminifera at varying temperatures in different seasons and years [21], (2) uncertainties associated with the deconvolution of seafloor dissolution effects [18], and (3) the con-

sistency with which tests can be cleaned of contamination by diagenetic and detrital phases [22–25].

Because foraminifera grow their tests by sequentially adding chambers and new layers to existing chambers, individual tests may comprise a range of diverse compositions that reflect changing habitat and seawater conditions during an individual foraminifer's lifetime [26]. Indeed, many species migrate through the water column, initially as juveniles into warmer surface waters and with maturity into deeper colder water to reproduce [26]. Most planktonic species also add a final, often thick, outer calcite crust (or 'gametogenic crust') in deeper colder water immediately prior to reproduction and ensuing death [26,27]. Electron-probe microanalysis studies have confirmed the presence of relatively Mg-poor, outer-wall layers in the tests of *Globorotalia truncatulinoides* [28], *Globorotalia tumida* [17], and *Globigerina bulloides* [7], consistent with the growth of final outer calcite crusts on these species in much colder water. Significant Mg concentration variation, albeit spatially incoherent, has been reported in *N. pachyderma* [29]. Systematic Mg-enrichment has been documented toward test exterior surfaces across the final outer crusts that have been precipitated by *G. sacculifer* in laboratory-culture experiments [1]. Reduction in bulk test Mg/Ca composition with partial seafloor dissolution indicate *G. sacculifer* grow more Mg-depleted, final outer-crust compositions in deeper colder water [11]; however, no significant Mg variability was found in an electronprobe study of fossil *G. sacculifer* tests [17]. Changes in bulk test compositions with progressive seafloor dissolution also provide qualitative evidence for the existence of significant compositional heterogeneity between and/or within tests in species that include *G. ruber*, *N. dutertrei*, and *G. tumida* [15,17,18]. Collectively, these results point to the occurrence of significant compositional heterogeneity within the tests of many planktonic foraminifera species, and indicate the interpretation of bulk test Mg/Ca compositions may not be straightforward. Furthermore, the conventional bulk analysis approach to foraminiferal seawater thermometry potentially averages significant compositional heterogeneity and, in so doing, may destroy a valuable record of seawater temperature variation in time and space.

3. Experimental method

We have employed a high-resolution LA-ICP-MS depth-profiling technique to investigate the nature and extent of compositional variation within the tests of a number of planktonic foraminifera species that are commonly used for palaeocean reconstruction, including *N. dutertrei*, *N. pachyderma*, *G. ruber* and *G. sacculifer*. Fossil tests of each species were obtained from a small number of deep-sea cores (see Table 1 for core and sample details) and analysed after cleaning by repeated rinsing and ultrasonication in ultrapure water (>18 MΩ) and AR-grade methanol to remove adhering detrital material (the latter confirmed by subsequent inspection of tests using scanning electron microscopy, SEM). Modern *G. ruber* tests, sampled by plankton tow, were also analysed following treatment in AR-grade H_2O_2 to remove organic material and applying the same cleaning procedures used for fossil tests.

Highly controlled and precise test sampling is achieved using a pulsed ArF Excimer laser ($\lambda = 193$ nm) fitted with simple image-projection optics [30]. It should be noted that poor absorption and catastrophic ablation of calcite occur with use of significantly longer-wavelength laser light [31]. In this regard, the capabilities of our laser sampling system are demonstrated by the generation of flat-bottomed pits in gem-quality calcite after application of 10 and 100 laser pulses (Fig. 1A,B). Each laser pulse shaves a uniform, ~ 0.1 μm thick, layer from the calcite sample surface and the application of multiple laser pulses proceeds with preservation of original subtle surface features down to a depth of about 5μm (Fig. 1A,B). Approximately 50% higher ablation rates are observed under the same conditions in foraminiferal calcite, based on ablation experiments conducted on the smooth-walled planktonic species *Pulleniatina obliquiloculata* (Fig. 1C,D). However, due to reduced laser fluence and increased reflection at inclined surfaces, uniform ablation

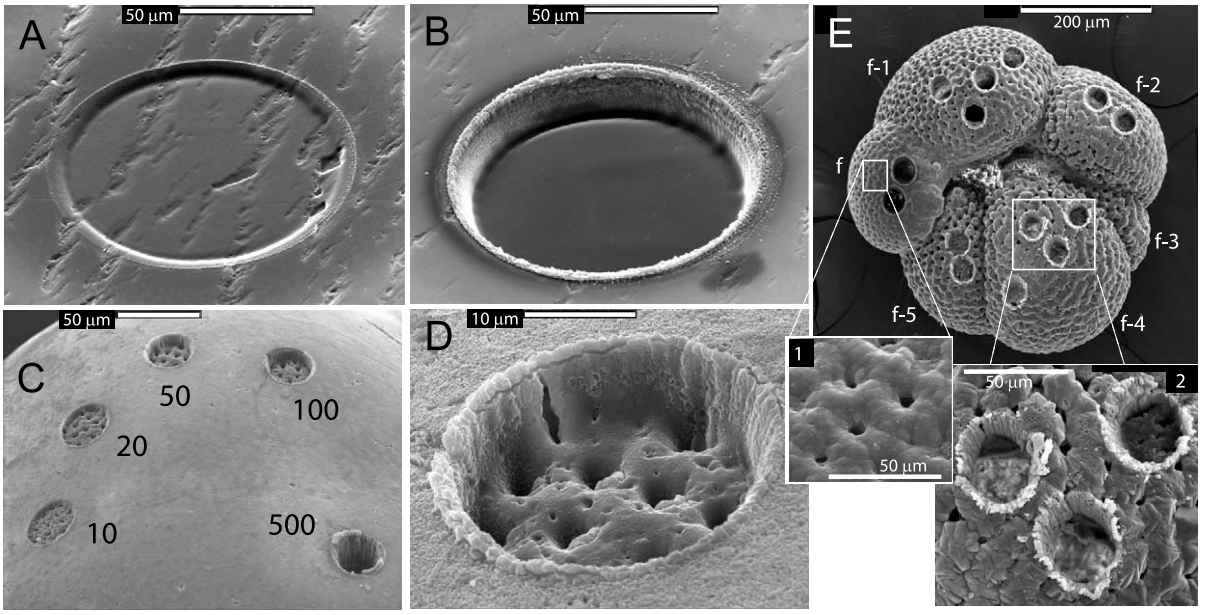

Fig. 1. SEM images of laser ablation pits formed in (A,B) gem-quality Iceland spar using 10 and 100 laser pulses, and (C) a fossil *P. obliquiloculata* test by 10, 20, 50, 100 and 500 laser pulses using a laser fluence of 5 J/cm^2. (D) Detail of the 50 pulse pit shown in panel C, which is approximately 7.5 μm deep. (E) A fossil *N. dutertrei* test, in which 14 separate composition profiles have been analysed by LA-ICP-MS and up to four replicates on each chamber. Inset E(1) shows detail of the reticulate surface texture present on the final chamber. Inset E(2) shows detail of 30 μm diameter pits in chamber f-4 and the surrounding blocky calcite textured test surface. Labels f, f-1, f-2, etc. indicate the chamber calcification order, counting back from the final chamber (f). Note scale bars.

does not occur across the target site in planktonic species with outward-opening pore structures (e.g. *G. sacculifer*; see Fig. 2). SEM images reveal that laser sampling proceeds through the test wall in these species by preferentially sampling outer layers from the tops of interpore ridges and spine bases, before developing more flat-bottomed pits and removing inner layers from deeper within test walls (Fig. 2).

Multiple trace elements are simultaneously profiled during laser sampling through individual chamber walls by repeated, rapid sequential peak hopping (dwell time = 30 ms) between selected isotopes (^{24}Mg, ^{25}Mg, ^{43}Ca, ^{44}Ca, ^{55}Mn, ^{68}Zn, ^{88}Sr, ^{138}Ba) using a quadrupole ICP-MS (Agilent 7500s). The ICP-MS is optimised for sensitivity across the analyte mass range subject to maintaining $ThO^+/Th^+ < 0.5\%$. Data reduction follows established protocols for time-resolved analysis [32]. This involves initial screening of spectra for outliers, followed by subtraction of mean background intensities (measured with the laser off) from analyte isotope intensities. Quantification is performed by external calibration using NIST610 and NIST612 glass standard reference materials and correction for yield variation by ratioing to an internal standard isotope (^{43}Ca) measured during each mass spectrometer cycle (~0.25 s). Internal standardisation using ^{43}Ca avoids detector non-linearity effects that can be encountered with higher-intensity ^{44}Ca signals in the analogue detection mode. Measured ^{44}Ca/^{43}Ca ratios on the NIST glasses and foraminiferal calcite are found to be equivalent within analytical uncertainty, indicating that interference of $^{27}Al^{16}O$ on ^{43}Ca and $^{12}C^{16}O_2$ on ^{44}Ca during NIST glass and calcite analysis, respectively, contribute biases of less than 0.5%.

Optimum spatial resolution is achieved by ablating small-diameter (30 or 40 μm) spots at 2 or 3 laser pulses per second using a moderately low laser fluence (5 J/cm^2), and by minimising

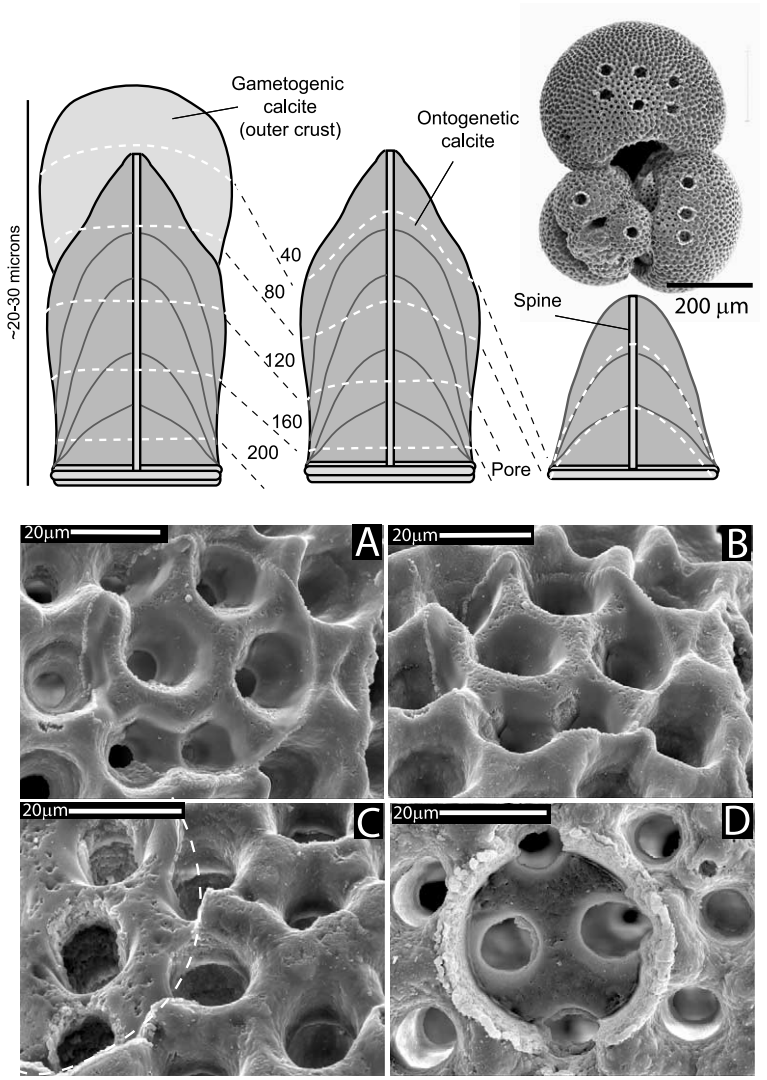

Fig. 2. SEM images and a schematic cross-section illustrating the effects of test surface topography on laser ablation pit development in *G. sacculifer* (an adult test with multiple ablation pits is shown at the upper right for reference). SEM images A and B show details of 30µm diameter pits formed by 20 and 40 laser pulses, respectively, and images C and D show the formation of deeper and flatter-bottomed pits by the application of 100 and 200 laser pulses. Note scale bars and the dashed white line in image C, which outlines the ablation pit periphery. These SEM images demonstrate the preferential ablation of material from surfaces that lie orthogonal to the incident laser beam, which results in greater ablation from the tops of interpore ridges and spine bases, and the development of increasingly flatter-bottomed pits as ablation progresses into the test wall. A schematic cross-section through interpore ridges that form *G. sacculifer* test walls illustrates the construction (right to left) of chamber walls by the addition of ontogenetic calcite layers to form the inner wall (dark grey with solid dark lines) and capping of ridges and spine bases by the final, outer (gametogenic) calcite crust (adapted from figure 6 in [27]). Dashed lines indicate the recession of the test surface with increasing numbers of laser pulses (values associated with adjacent dashed lines). Note scale bars on both the SEM images and the schematic cross-section.

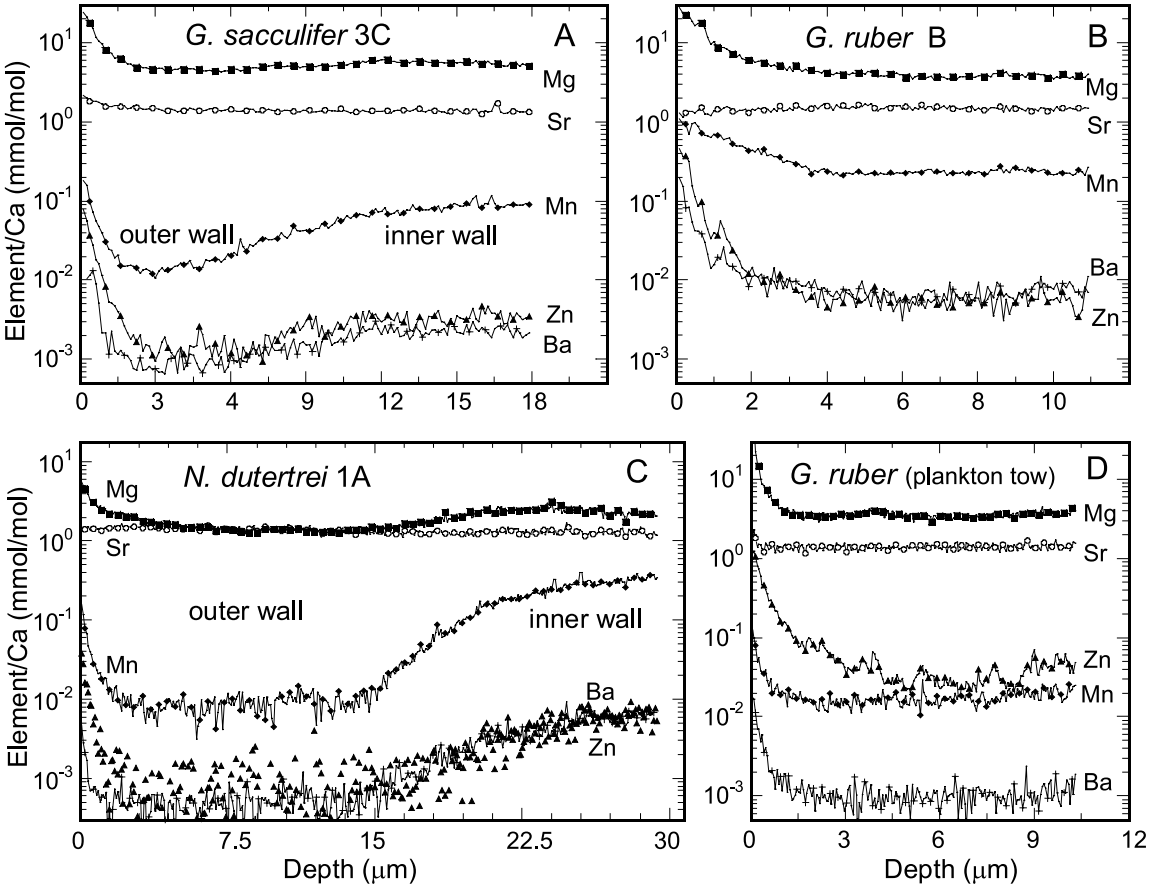

Fig. 3. Trace element compositional profiles through the test walls of fossil specimens of (A) *G. sacculifer*, (B) *G. ruber*, (C) *N. dutertrei* (same specimen as shown in Fig. 1), and (D) a modern *G. ruber* test that was sampled by plankton tow. Measured metal/Ca molar ratios are plotted on a log scale, and the profile depth is calculated from the number of laser pulses applied, assuming an ablation rate of 0.15 μm per pulse based on measured rates of ablation of *P. obliquiloculata* tests (see Fig. 1C,D). Note the narrow zone of Mg–Mn–Zn–Ba enrichment that occurs at the external surface (0 μm in all profiles) of each chamber and the development of distinct inner- and outer-wall layers in *G. sacculifer* and *N. dutertrei* profiles. Test sample numbers follow the species name.

mean particulate residence times ($t_{1/2} \sim 0.35$ s) in the ablation cell volume following each laser pulse. These short residence times are facilitated by a two-volume ablation cell design that incorporates a small ablation volume (~ 2 cm^3), which is effectively isolated from a much larger ($10 \times 10 \times 3$ cm) volume containing samples and standards. This unique design also avoids cross-contamination between samples and standards by ablation products that can be widely dispersed beyond the immediate ablation environment in simpler, single-volume ablation cell designs. Each analysis consumes only 10–20 ng of test material, or about 0.1% of the total test mass, and typically requires between 20 and 60 s, depending on test wall thickness. Multiple profiles can be obtained from individual chambers of a single test (Fig. 1E) and several hundred chamber-wall profiles can be acquired in a day.

4. Results

Compositional profiles that illustrate the range of chemical variation found through the test walls of the analysed foraminifera species are shown in

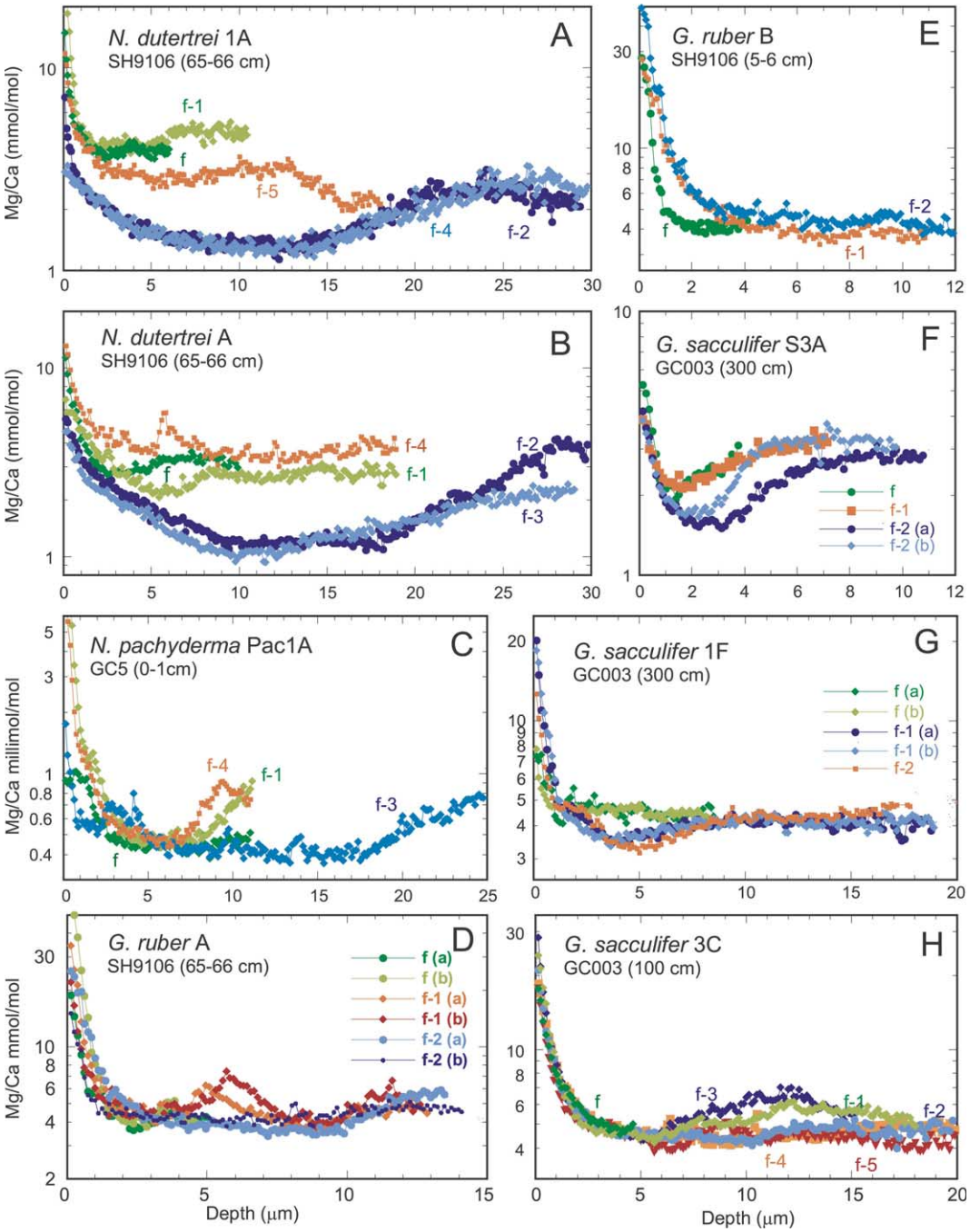

Fig. 4. Compositional profiles showing the variation of Mg/Ca molar ratios through each analysed chamber wall of individual tests of (A,B) *N. dutertrei*, (C) *N. pachyderma*, (D,E) *G. ruber*, and (F–H), *G. sacculifer* (note the vertical log scale, and profile depth has been calculated as in Fig. 3). Observe that the different species display characteristic profile forms and compositions, and in the case of *N. dutertrei*, systematic variation of profile forms and thickness with chamber calcification order. Further note the thin Mg-rich external surfaces present at the beginning of all wall profiles, and the development of low-Mg outer-wall (crust) layers in some *G. sacculifer* tests. Labels f, f-1, f-2, etc. indicate the chamber calcification order, counting back from the final chamber (f). The reproducibility of profiles is indicated by replicate profile analyses (denoted a and b) made on the same chamber (see panels D, F and G). Test sample numbers follow the species name.

Fig. 3. Measured trace element concentrations are consistent with abundance ranges reported previously for planktonic foraminifera [8]. Mg, Mn, Zn, and Ba are notable for their systematic, large and correlated variation through test walls, whereas Sr shows unrelated, comparatively uniform distributions. To help clarify the subsequent discussion of these composition profiles, we use the term 'surface veneer' to refer to the thin Mg–Mn–Ba–Zn enrichments that occur at the beginning of each compositional profile and coincide with the test outer surface. The terms 'outer wall' and 'inner wall' are used to distinguish between distinct layer compositions, where developed, within test walls.

Thin (typically <1–3 μm) Mg-, Mn-, Zn- and Ba-rich surface veneers are observed on all chambers and all tests of each species analysed. Comparable trace element-rich surface veneers are also present on *G. ruber* tests sampled by plankton tow (Fig. 3D). Close examination of the profiles in Fig. 3C,D reveals variation in the width and form of the surface enrichment for different elements. For example, the zone of anomalous Mn, Ba and Zn enrichment in the *N. dutertrei* test profile shown in Fig. 3C is only 1–2 μm thick, whereas Mg increases toward the test surface in this profile over a distance of almost 10 μm (see profile f-2 in Fig. 4A for greater detail).

Compositionally distinct inner-wall and outer-wall layers, of varying relative thickness, are observed in several species, particularly *N. dutertrei* and often also *N. pachyderma* and *G. sacculifer* (Figs. 3 and 4). Where present, inner-wall layers are usually enriched in Mg and other trace elements (except Sr) but these enrichments do not occur to the same extent, nor do they match in detail the characteristics of the surface veneers. The relative thickness of the inner- and outer-wall layers differs between species, and in the case of *N. dutertrei* tests also varies significantly between chambers (see Figs. 3C and 4A,B). The latter compares to *G. sacculifer* tests where low Mg outer-wall layers, although not always evident (Figs. 3A and 4F–H), tend to be of similar thickness and to comprise a relatively small proportion (25–50%) of the total wall thickness in most chambers. The often complex multi-layered wall profiles of these two species contrast with the relatively simple profiles of *G. ruber*, which are characterised by strong asymmetry due to the presence of surface veneers but otherwise exhibit comparatively uniform internal wall compositions (Figs. 3B,D and 4D,E). Furthermore, Mg/Ca composi-

Table 1
Deep-sea core and plankton tow details

Core ID	Location	Latitude and longitude	Depth below seafloor (m)	Interval below seafloor (cm)	Species and size range (μm)	Age[a] (yr BP)	Modern mean annual SST [33] (°C)
SH9016	Timor Sea	8°27′S, 128°14′E	1805	5–6	*N. dutertrei*, *G. ruber*, 300–450	1 711	28.2
				65–66		19 323	
RS122/GC/003	Cartier Trough, Timor Sea	11°28′S, 124°35′E	416	97.5–102.5	*G. sacculifer*, 350–550	∼6 000[b]	28.6
				297.5–302.5		18 140	
GC5	Prydz Bay	67°04′S, 69°01′E	320	0–1	*N. pachyderma*, 250–350		−0.6
Plankton tow			Depth below sea surface				Measured seawater temperature
Fr2/96-station 5	Offshore Western Australia	28°43′S, 113°24′E	0–60		*G. ruber*, 350		26.5, 26.0 at 60 m

[a] Ages are radiocarbon years determined by accelerator mass spectrometry.
[b] Age inferred on the basis of 6664 yr BP age at 110 cm.

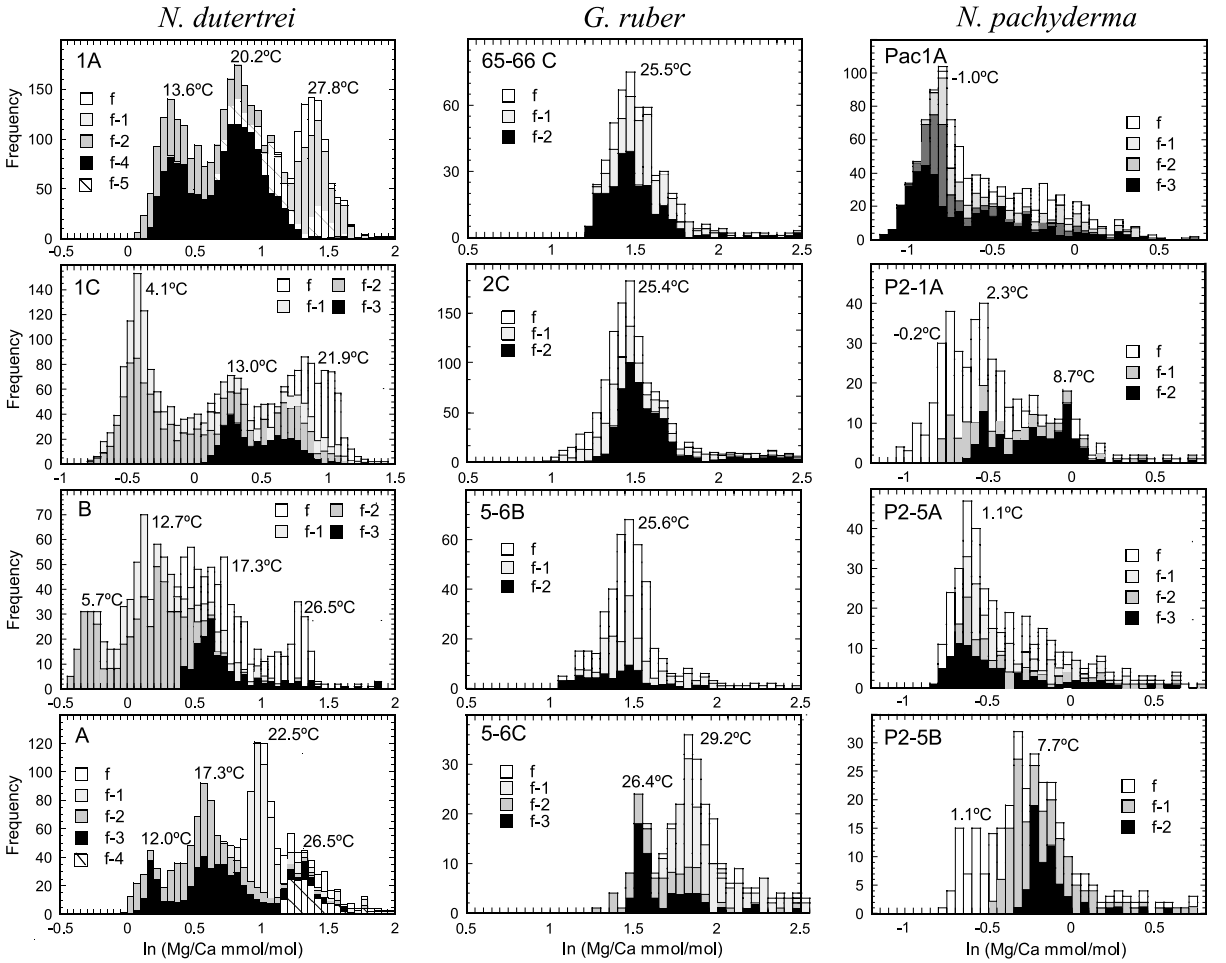

Fig. 5. Histograms of the natural logarithm of individual (Mg/Ca) mmol/mol ratios compiled from the profiled compositions of each analysed chamber of individual tests of *G. ruber*, *N. pachyderma* and *N. dutertrei*. Note that calcification temperatures vary linearly with ln(Mg/Ca), and have been estimated for *G. ruber* using the calibration reported for this species by Rosenthal and Lohmann [17], by applying a nominal shell weight of 11 μg to avoid calibration bias related to seafloor dissolution. Calcification temperature estimates for *N. pachyderma* and *N. dutertrei* have been calculated using the multi-species calibration of Nürnberg et al. [2], following adjustment for original electron-probe analytical bias relative to ICP techniques [5]. f, f-1, f-2, etc. denote the different chamber compositions in each test (see Fig. 1 for notation). Note the distinctive Mg/Ca distribution characteristics of the different species (see text for discussion). The *N. dutertrei* and the upper two *G. ruber* tests are from an LGM sample interval in core SH9106, the lower two *G. ruber* tests from a Holocene sample interval in the same core, and the *N. pachyderma* are from core GC5. See Table 1 for core location, interval ages, and sample details. The test sample number is indicated above the legend in each panel.

tions and profile forms tend to be similar in all chambers of *G. ruber* and *G. sacculifer*, whereas large differences are observed between chambers in *N. dutertrei* (Fig. 4A,B) and occasionally also in *N. pachyderma* (Fig. 4C).

The nature and extent of compositional variability within and between tests of the different species can be most readily appreciated and assessed using histograms that compile the individual Mg/Ca measurements that form the compositional profiles obtained from each chamber in each test (Figs. 5 and 6). These histograms exhibit a range of characteristic, and often different, forms for each species. *N. dutertrei* tests exhibit

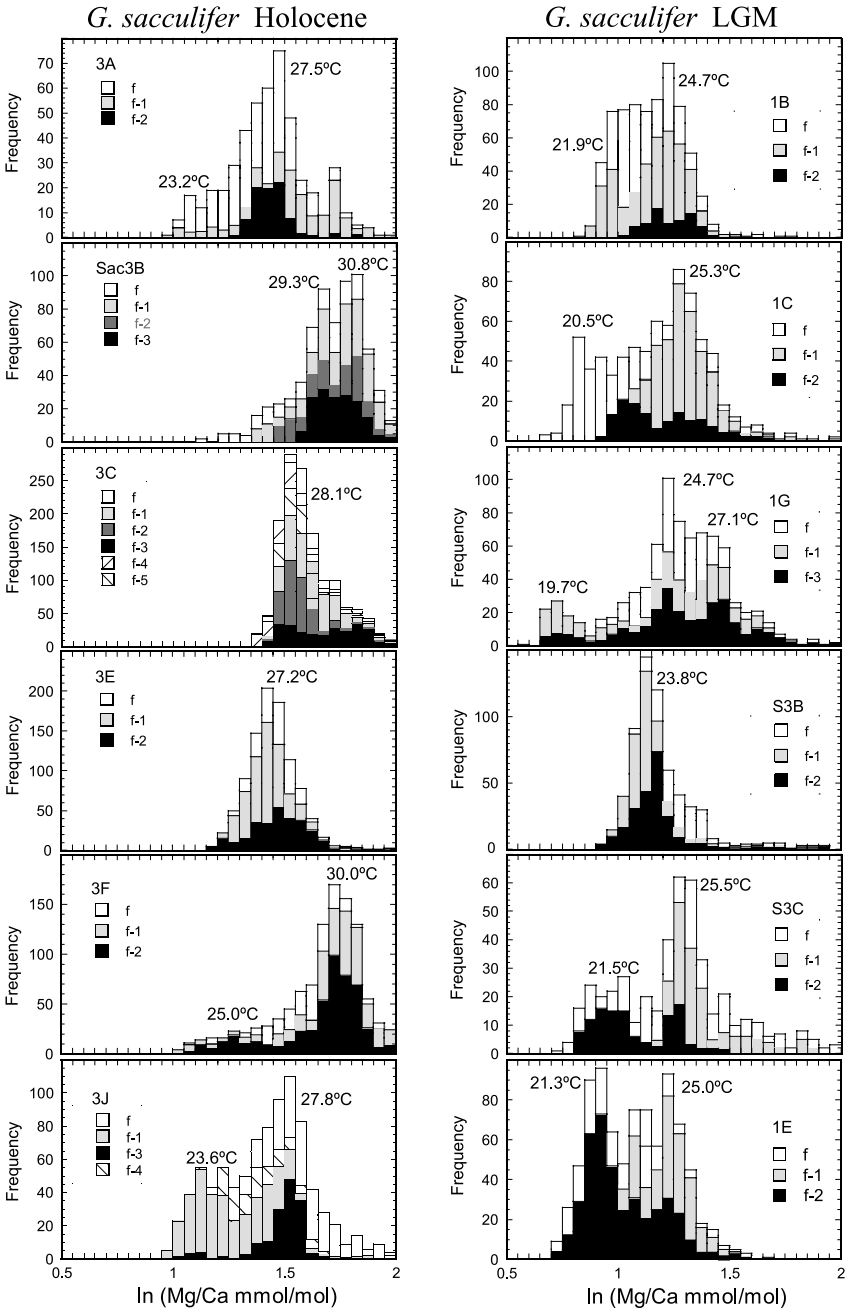

Fig. 6. Histograms of the natural logarithm of individual (Mg/Ca) mmol/mol ratios compiled from the profiled compositions of each analysed chamber of individual *G. sacculifer* tests. Note the variation in distribution forms in this species, which range from simple unimodal to bimodal distributions that have a characteristic dominant mode with higher Mg/Ca. Tests from an early- to mid-Holocene interval in the core RS122/GC/003 are shown on the left and from an LGM interval on the right (see Table 1 for core location, interval ages and sample details). Calcification temperature estimates have been calculated using the *G. sacculifer* calibration of Rosenthal and Lohmann [17], by applying a nominal shell weight of 45 μg to avoid calibration bias related to seafloor dissolution. Note the lower overall temperatures recorded by the LGM tests. f, f-1, f-2, etc. denote the chamber compositions (see Fig. 1 for notation). Test sample numbers are above the legend in each panel.

the largest Mg/Ca compositional range (typically spanning 1.5–2 natural log units) and possess complex distributions with three or more well developed modes. Much simpler distributions are observed in other species, in particular *G. ruber*, which is notable for its tight, usually unimodal distributions that tend to be skewed toward higher Mg/Ca values by the Mg-rich surface veneers. Much broader unimodal distributions that are often strongly positively skewed are characteristic of some but not all *N. pachyderma* tests from Prydz Bay. Simple tight unimodal distributions, similar to those of *G. ruber*, are observed in some *G. sacculifer* tests, but many have either a secondary mode at lower Mg/Ca or a tail toward lower Mg/Ca compositions. The multiple composition modes that are observed in all *N. dutertrei* and many *G. sacculifer* tests (Figs. 5 and 6), and occasionally in other species, are typically associated with specific chambers or groups of chambers. In some cases, individual chambers are represented in more than one Mg/Ca composition mode, this being a reflection of the development of compositionally distinct inner- and outer-wall layers in these chambers.

The observed compositional range and the spacing of Mg/Ca modes in the individual tests in Figs. 5 and 6 are related linearly to calcification temperature through the exponential form of foraminiferal Mg/Ca seawater thermometers. Accordingly, we have derived temperature estimates for each Mg/Ca mode in each test by applying thermometer calibrations that are (as far as possible) appropriate for each species and that are free of dissolution-related biases (see captions to Figs. 5 and 6 for details). The temperatures obtained for the primary composition modes of the *G. sacculifer*, *G. ruber* and *N. pachyderma* tests, and the highest Mg/Ca composition modes observed in the *N. dutertrei* tests, are notable for being broadly consistent with present-day, mean annual SSTs for the deep-sea core locations from which these tests originate (i.e. 28.6 and 28.2°C for cores RS122/GC/003 and SH9016 in the Timor Sea, and −0.6°C for GC5 in Prydz Bay [33]). However, all the *N. dutertrei* tests and half the *G. ruber* and *G. sacculifer* tests are derived from Last Glacial Maximum (LGM) core intervals, and the remaining *G. ruber* and *G. sacculifer* tests are from early to mid-Holocene core intervals (see Table 1 for details). In this context, the LGM *G. sacculifer* tests are notable for clustering within a lower temperature range (23.8–25.5°C) than their Holocene counterparts (27.2–30.8°C), and three of four LGM *G. ruber* tests for registering temperatures near 25.5°C (one at 29°C) whereas three of four Holocene tests register near 29°C (the other, #5-6B, 25.6°C; Fig. 6). These estimates suggest calcification temperatures for LGM tests that are on average about 3.5°C lower than Holocene tests of the same species. This temperature difference is slightly higher than the estimated change in SST in the tropical eastern Indian Ocean between the LGM and today (i.e. 1–2°C), based on application of the Modern Analogue Technique to planktonic foraminifera assemblages [34]. The temperature ranges recorded by the differing primary Mg/Ca composition modes of the Holocene and LGM *G. sacculifer* tests (i.e. 27.2–30.8°C and 23.8–27.1°C) are in keeping with the magnitude of modern, average monthly SST variation at the RS122/GC/003 core site (i.e. 26.7–29.9°C [33]). Similar ranges, spanning about 3.5°C, are also observed for the smaller numbers of Holocene and LGM *G. ruber* tests from SH9016, which has a modern, average monthly SST range from 26.7 to 29.5°C [33].

The highest Mg/Ca composition modes of the LGM *N. dutertrei* tests are notable for having temperature estimates that are on average about 2–3°C higher than LGM *G. ruber* and *G. sacculifer* tests. This suggests the thermometer applied to these tests [2] may be overestimating these calcification temperatures for *N. dutertrei* by several degrees.

The large spread in Mg/Ca compositions and the lower Mg/Ca composition modes that are observed in *N. dutertrei* and many *G. sacculifer* tests range to significantly cooler temperatures than the near-SST estimates that are recorded by the highest Mg/Ca modes in the same tests. The intermediate Mg/Ca compositions that dominate most *N. dutertrei* tests correspond to temperature estimates in the range 12–23°C; however, temperatures below 13°C and as low as 4°C are indicated for the lowest Mg/Ca mode compositions in this

species. The secondary, lower Mg/Ca composition modes that are observed in many *G. sacculifer* tests, which are a manifestation of low-Mg outer-wall layer development, register calcification temperatures between 3 and 7.5°C lower than the principal Mg/Ca composition modes in these tests. The compositions of these low-Mg outer-wall layers reflect calcification temperatures between 20 and 22°C in LGM tests, and between 23 and 25°C in Holocene tests (see Fig. 6).

The anomalously high Mg/Ca compositions of the surface veneers that have been documented on all tests correspond to calcification temperature estimates that greatly exceed acceptable limits (i.e. SSTs at each core locality). The *N. pachyderma* tests from Prydz Bay (Fig. 5) are further notable for exhibiting a range of Mg/Ca compositions that extends well beyond acceptable calcification temperatures for this locality (both the monthly mean SST range and variation with depth span only −1.3 to 0.5°C [33]). Different chambers in the same test also often have very distinct compositions, with final chambers usually having the lowest Mg/Ca.

5. Discussion

The Mg/Ca and other trace element compositional variability that we have documented in planktonic foraminifera tests, considerably extends current knowledge of the nature and extent of compositional variability within several key species that are widely used in palaeoceanographic reconstruction. Our results demonstrate for each analysed species that bulk pooled test compositions are likely to integrate diverse compositional variation that occurs both within and between tests. Furthermore, comparison with present-day seawater temperatures indicates that reasonable calcification temperature estimates may be obtained from each analysed species using LA-ICP-MS. However, the high Mg/Ca compositions found in parts of many *N. pachyderma* tests from Prydz Bay and the Mg-rich surface veneers that have been observed on all analysed tests correspond to unacceptably high calcification temperatures.

5.1. Origin of Mg-rich test surfaces

The presence of similar, if not identical, Mg-rich surface veneers on both modern (plankton tow-sampled) tests and fossil tests suggests this Mg enrichment may be of primary biogenic origin. In support of this possibility we note that Bé [27] reported the precipitation of thin (∼0.2 μm), smooth-surfaced, veneers upon the terraced pre-gametogenic shell surfaces of *G. sacculifer*, and SEM images (see Plate IX in [27]) revealed these thin surface veneers to be preferentially removed by seafloor dissolution, indicating they are likely to be more Mg-rich than underlying pre-gametogenic calcite. Brown and Elderfield have also observed, in their seminal paper on the effects of seafloor dissolution [17], that both the outer surfaces and inner walls of fossil *G. sacculifer* tests are first affected by seafloor dissolution. Moreover, the large Mg enrichments documented to occur toward test surfaces across the final outer crusts of laboratory-cultured *G. sacculifer*, indicates that anomalous, Mg-rich calcite compositions can be precipitated under physiological control by this species [1]. Collectively these observations lend support to the possibility that anomalous, Mg-rich calcite could be precipitated during the final stages of test calcification, although the reasons why this may occur are unclear (see also [1]).

On the other hand, if adhering Mg-rich clays, carbonates, organic material or other phases are responsible for the Mg-rich surface veneers we are able to provide some useful constraints on their nature. In this regard, the test surfaces are notable for reaching Mg-rich calcite compositions (< 1–6 mol % $MgCO_3$) and for having elevated yet still trace level concentrations of Mn, Zn and Ba (Figs. 3). These relatively low Mn concentrations are inconsistent with the Mn–Mg–CO_3 coatings that were originally suggested to develop on fossil tests during diagenesis below the Mn-reduction front in seafloor sediments [22]. Furthermore, the Mg-rich surface enrichment and the observed Mg distribution across chamber walls is unlikely to reflect residual Mg-rich organic matter upon and within tests (see also [24]), as indicated by the failure of strong oxidants to remove Mg-rich

surfaces from live-sampled *G. ruber* tests and the very acceptable temperature estimates that are calculated for wall interiors based on measured Mg/Ca concentrations. Integration of wall composition profiles, to both include and exclude the Mg-rich test surfaces, indicates they bias whole-test compositions toward higher Mg/Ca values by between 5 and 35%, which is broadly consistent with the extent to which bulk test compositions are lowered by test cleaning procedures (e.g. [6]).

5.2. Calcification conditions for different test components

The distribution of Mg within test wall interiors, in particular the depletion of Mg in the outer-wall layers of *N. dutertrei* and many *G. sacculifer* tests, is consistent with previously documented low-Mg outer-crust development in *G. bulloides* and Globorotalid species, and documents directly, for the first time, the calcification of low-Mg final outer-crust compositions in *G. sacculifer*. Interestingly, inspection of the *N. dutertrei* profiles shown in Fig. 5 reveals that the low-Mg outer-wall layer compositions are inconsistently developed on different chambers in the same test, with particularly thick and Mg-poor layers (comprising >60–70% of the wall width) occurring on only a few chambers (usually f-2, f-3 or f-4; see Fig. 1 for chamber notation). The very low calcification temperatures (between 4 and 13°C) estimated from the compositions of these outer crusts correspond to present-day temperatures at depths below 225 m and as deep as 1100 m at the SH9016 core site [33]. This compares to the intermediate Mg/Ca compositions that dominate most tests, which reflect warmer temperatures (12–23°C) that correspond to the approximate position of the present-day main thermocline, between 100 and 250 m [33]. In contrast to *N. dutertrei*, the low-Mg outer-wall compositions in *G. sacculifer* tests comprise a relatively small proportion of the total wall thickness (typically between 20 and 50%), and record calcification temperatures that are between 3 and 7.5°C lower than the primary Mg/Ca mode temperatures of the same tests. For Holocene *G. sacculifer* tests, estimates of the outer-crust calcification temperature range between 23 and 25°C. This corresponds to present-day mean annual temperatures at water depths between 70 and 100 m at the RS122/GC/003 core site [33]. Among the small number of *G. ruber* tests analysed in this study, several show significant Mg/Ca variation that is manifested as compositionally distinct chambers and also, outer- and inner-wall layers in some chambers. The bimodal Mg/Ca distributions observed in two tests (one of which is illustrated in Fig. 5) indicate a calcification temperature difference of order 2–3°C. Indeed, the limited calcification temperature range of *G. ruber* tests, as evidenced by their tight Mg/Ca composition distributions, is consistent with the exclusively near-surface habitat of this species (e.g. [26]). Nonetheless, our results suggest some *G. ruber* may calcify over a small but significant depth range, sufficient to encounter a 2–3°C temperature variation.

The reason for the anomalously high temperature estimates (in the range 7–8°C) that have been obtained for parts of *N. pachyderma* tests from Prydz Bay is unclear, and suggests that variation in calcification kinetics, other physiological controls, or possibly salinity changes, could dominate over temperature control at very low temperatures.

5.3. Reconstruction of habitat migration

The ability to measure compositional variation within the sequentially precipitated components (chambers and wall layers) that form single tests presents the possibility of being able to reconstruct habitat migration during the adult life-cycle stages of individual foraminifera. In the case of *G. sacculifer* tests this is relatively straightforward, with the low Mg/Ca crusts that are developed on many tests indicating descent from near-surface conditions to undergo final calcification at temperatures in the range 23–25°C. The latter corresponds to depths between 70 and 100 m, given early- to mid-Holocene ocean temperatures are comparable to the present-day one at the RS122/GC/003 core site [33]. The temperature of final outer-crust growth is similar to estimates based on seafloor dissolution effects upon bulk

G. sacculifer test compositions from the tropical Atlantic (i.e. 21 ± 1.5°C), for which corresponding depths ranged between 100 and 225 m, east to west, across the tropical Atlantic [11]). These and our depth estimates are significantly shallower than some previously reported estimates (i.e. >200 m in the Red Sea [35], 300–800 m [36]).

The record of calcification temperature contained in *N. dutertrei* tests is considerably more complex than in *G. sacculifer*. Using the test illustrated in Fig. 1E as an example, for which profiles are shown in Figs. 3C and 4A, it can be seen that the more Mg-rich composition of the final two chambers (f and f-1) compares closely to the inner-wall layers of earlier formed chambers (particularly f-2 and f-4). Calcification temperature estimates for the final two chambers (f and f-1) in this test are near 27.8°C (see Fig. 5, top left histogram), whereas temperatures of 20 and 13.5°C are observed for the inner- and outer-wall layers of chambers f-2 and f-4, respectively, and 20–28°C for chamber f-5. The greater thickness and coarse, euhedral, calcite surface textures of chambers f-2 and f-4 (Fig. 1E) indicate final crust development was concentrated on the exterior of these chambers, and the low Mg/Ca compositions of these crusts indicate they grew under much colder conditions than other test components. Further note that the surface texture variations on the different chambers of this test are also consistent with the documented development of reticulate and crystalline (euhedral calcite) surface textures in this species under warmer and colder conditions, respectively [37]. We interpret the Mg/Ca variation observed within this test to reflect calcification of earlier chambers, f-5 through f-2, under relatively cool conditions (~20°C) in the upper thermocline, prior to migration into warmer (~27.5°C) near-surface waters, where the final two chambers were added, followed by rapid descent into much colder (<14°C) water near the base of the thermocline, where the final outer calcite crust was added. Other *N. dutertrei* tests show a similar pattern of Mg/Ca variation in sequentially precipitated test components (Fig. 5) that also reflect initial residence above or within the upper thermocline, followed by descent to depths near the base or below the thermocline. This migration pattern is compatible with existing knowledge of the life-cycle of *N. dutertrei* based on plankton tow and sediment trap studies, which indicate this species resides predominantly in or above the thermocline subject to the position of the chlorophyll maximum and that reproduction occurs deeper within the thermocline [38,39]. Despite the limited nature of these results they demonstrate the potential power of using LA-ICP-MS microanalysis to trace habitat changes during the adult life-cycle stages of planktonic foraminifera. They also highlight the fact that such habitat changes can produce very large Mg/Ca variations within individual tests, particularly in species that migrate large vertical distances in the water column. Understanding the impact these habitat changes have on test Mg/Ca and $\delta^{18}O$ composition is required if reliable reconstructions of palaeocean conditions are to be made using such species.

5.4. *Application of LA-ICP-MS to palaeocean reconstruction*

The results of this study provide 'proof of concept' that LA-ICP-MS may be used to extract records of past ocean temperature from fossil planktonic foraminifera tests. Compared to conventional bulk analysis this technique offers significant advantages through its potential to derive the range and variability of seawater temperature, in addition to a simple mean value, from a population of fossil tests. Improved constraints on thermocline structure and depth could potentially also be obtained from analysis of sequentially precipitated test components in species that migrate through significant vertical ranges. Moreover, sample preparation is straightforward, and contributions from anomalously Mg-rich surface coatings (whatever their origin) can be readily excluded from the analysis without invoking complex and time-consuming cleaning procedures. LA-ICP-MS can also analyse multiple trace elements in addition to Mg/Ca (e.g. Sr, Zn, Ba, Cd) and, perhaps most significantly, allows for subsequent $\delta^{18}O$ analysis of the same test material, and possibly more precise and accurate con-

straints to be placed on palaeo-salinity and seawater density.

6. Summary

Systematic large and correlated variation of Mg/Ca, Mn/Ca, Ba/Ca and Zn/Ca but relatively uniform Sr/Ca has been documented within the test walls of several planktonic species (*G. sacculifer*, *G. ruber*, *N. pachyderma* and *N. dutertrei*) by high-resolution depth profiling using LA-ICP-MS. Distinct chamber and wall layer compositions can be resolved using this technique, and compositional variation associated with sequentially precipitated test components can be quantified. The variation observed within tests of the analysed planktonic species is found to be consistent with seawater temperature and associated habitat changes experienced during the adult stages of these species (with the notable exception of *N. pachyderma*, which exhibits Mg/Ca variation extending well beyond that able to be explained by temperature variation alone). Shallow-dwelling species, in particular *G. ruber*, but also *G. sacculifer*, tend to have more uniform chamber and wall layer compositions than deeper-dwelling species, such as *N. dutertrei*. Low-Mg/Ca outer-wall layer compositions developed on *G. sacculifer* and *N. dutertrei* tests are consistent with final outer-crust growth on these species near the top of the thermocline and at the base and below the thermocline, respectively. The Mg-rich calcite (<1–6 mol% Mg) veneers that are observed on the external surfaces of both fossil and modern tests are of uncertain but possible biogenic origin. These Mg-rich surface coatings bias bulk test compositions toward higher Mg/Ca values by between 5 and 35%

LA-ICP-MS shows considerable promise as a means for reconstructing palaeo-seawater temperatures from fossil planktonic foramifera tests. This technique stands to add value to deep-sea core-derived palaeoceanographic and climate records by yielding (1) the range and variability of past seawater temperature from a population of tests, and (2) insights into thermocline depth and structure by analysis of specific test parts in species that migrate through large vertical ranges. The technique may also be used to track habitat changes that take place during the adult life-cycle stages of planktonic foraminifera.

Acknowledgements

We thank Michael Shelley for assisting with LA-ICP-MS analysis, Judith Shelley for picking foraminifera from deep-sea core material, George Chaproniere for confirming the identification of species and for discussing aspects of foraminifera ecology, and Wolfgang Müller for critical assessment of an early draft of this manuscript. We particularly wish to thank Dr. G.J. Reichart and two anonymous reviewers for critical reviews that have resulted in improvements to this manuscript.***[BARD]***

References

[1] D. Nürnberg, J. Bijma, C. Hemleben, Assessing the reliability of magnesium in foraminiferal calcite as a proxy for water mass temperature, Geochim. Cosmochim. Acta 60 (1996) 803–814.

[2] D. Nürnberg, J. Bijma, C. Hemleben, Erratum: Assessing the reliability of magnesium in foraminiferal calcite as a proxy for water mass temperature, Geochim. Cosmochim. Acta 60 (1996) 2483–2484.

[3] Y. Rosenthal, E.A. Boyle, N. Slowey, Temperature control on the incorporation of magnesium, strontium, fluorine, and cadmium into benthic foraminiferal shells from Little Bahama bank: prospects for thermocline paleoceanography, Geochim. Cosmochim. Acta 61 (1997) 3633–3643.

[4] D.W. Lea, T.A. Mashiotta, H.J. Spero, Controls on magnesium and strontium uptake in planktonic foraminifera determined by live culturing, Geochim. Cosmochim. Acta 63 (1999) 2369–2379.

[5] D. Nürnberg, A. Müller, R.R. Schneider, Paleo-sea surface temperature calculations in the equatorial east Atlantic from Mg/Ca ratios in planktic foraminifera: a comparison to sea surface temperature estimates from U^{K}_{37}, oxygen isotopes, and foraminiferal transfer function, Paleoceanography 15 (2000) 124–134.

[6] D.W. Hastings, A.D. Russell, S.R. Emerson, Foraminiferal magnesium in *Globigerinoides sacculifer* as a paleotemperature proxy, Paleoceanography 13 (1998) 161–169.

[7] H. Elderfield, G. Ganssen, Past temperature and $\delta^{18}O$ of surface ocean waters inferred from foraminiferal Mg/Ca ratios, Nature 405 (2000) 442–445.

[8] D.W. Lea, Trace elements in foraminiferal calcite, in: B.K. Sen Gupta (Ed.), Modern Foraminifera, Kluwer Academic, 1999, pp. 259–277.
[9] E.J. Rohling, S. Cooke, Stable oxygen and carbon isotopes in foraminiferal carbonate shells, in: B.K. Sen Gupta (Ed.), Modern Foraminifera, Kluwer Academic, 1999, pp. 239–258.
[10] T.A. Mashiotta, D.W. Lea, H.J. Spero, Glacial-interglacial changes in subantarctic sea surface temperature and δ^{18}O-water using foraminiferal Mg, Earth Planet. Sci. Lett. 170 (1999) 417–432.
[11] Y. Rosenthal, G.P. Lohmann, K.C. Lohmann, R.M. Sherrell, Incorporation and preservation of Mg in *G. sacculifer*: implications for reconstructing the temperature and $^{18}O/^{16}O$ of seawater, Paleoceanography 15 (2000) 135–145.
[12] G.A. Schmidt, Error analysis of paleosalinity calculations, Paleoceanography 14 (1999) 422–428.
[13] W.S. Broecker, Paleocean circulation during the last deglaciation: a bipolar see-saw?, Paleoceanography 13 (1998) 119–121.
[14] P.U. Clark, N.G. Pisias, T.F. Stocker, A.J. Weaver, The role of the thermohaline circulation in abrupt climate change, Nature 15 (2002) 863–869.
[15] P.S. Dekens, D.W. Lea, D.K. Pak, H.J. Spero, Core top calibration of Mg/Ca in tropical foraminifera: refining paleotemperature estimation, Geochem. Geophys. Geosyst. (2002) 3.
[16] D.W. Lea, D.K. Pak, H.J. Spero, Climate impact of Late Quaternary equatorial Pacific sea surface temperature variations, Science 289 (2000) 1719–1724.
[17] S.J. Brown, H. Elderfield, Variation in Mg/Ca and Sr/Ca ratios of planktonic foraminifera caused by postdepositional dissolution evidence of shallow Mg-dependent dissolution, Paleoceanography 11 (1996) 543–551.
[18] Y. Rosenthal, G.P. Lohmann, Accurate estimation of sea surface termperatures using dissolution corrected calibrations for Mg/Ca paleothermometry, Paleoceanography 17 (2002) 1044–1049.
[19] Y. Rosenthal, M.P. Field, R.M. Sherrell, Precise determination of element/calcium ratios in calcareous samples using sector field inductively coupled plasma mass spectrometry, Anal. Chem. 71 (1999) 3248–3253.
[20] S. deVilliers, M. Greaves, H. Elderfield, An intensity ratio calibration method for the accurate determination of Mg/Ca and Sr/Ca of marine carbonates by ICP-AES, Geochem. Geophys. Geosyst. 3,
[21] E.A. Boyle, Limits on benthic foraminiferal chemical analyses as precise measures of environmental properties, J. Foraminifer. Res. 25 (1995) 4–13.
[22] E.A. Boyle, Manganese carbonate overgrowths on foraminifera test, Geochim. Cosmochim. Acta 47 (1983) 1815–1819.
[23] E.A. Boyle, L.D. Keigwin, Comparison of Atlantic and Pacific paleochemical records for the last 215,000 years: Changes in deep ocean circulation and chemical inventories, Earth Planet. Sci. Lett. 76 (1985/86) 135–150.
[24] P.A. Martin, D.W. Lea, A simple evaluation of cleaning procedures on fossil benthic foraminiferal Mg/Ca, Geochem. Geophys. Geosyst. 3 (2002).
[25] B.A. Haley, G.P. Klinkhammer, Development of a flow-through system for cleaning and dissolving foraminiferal tests, Chem. Geol. 185 (2002) 51–69.
[26] C. Hemleben, Modern Planktonic Foraminifera, Springer, 1989, pp. 363.
[27] A.W.H. Bé, Gametogenic calcification in a spinose planktonic foraminifer, Mar. Micropaleontol. 5 (1980) 283–310.
[28] D.L. Duckworth, Magnesium concentration in the tests of the planktonic foraminifer *Globorotalia truncatulinoides*, J. Foraminifer. Res. 7 (1977) 304–312.
[29] D. Nürnberg, Magnesium in tests of *Neogloboquarina pachyderma* sinistral from high northern and southern latitudes, J. Foraminifer. Res. 25 (1995) 350–368.
[30] S.M. Eggins, L.K. Kinsley, J.M.G. Shelley, Deposition and element fractionation processes occurring during atmospheric pressure laser sampling for analysis by ICPMS, Appl. Surf. Sci. 127–129 (1998) 278–286.
[31] T.E. Jeffries, S.E. Jackson, H.P. Longerich, Application of a frequency quintupled Nd:YAG source ($\lambda = 213$ nm) for laser ablation ICP-MS analysis of minerals, J. Anal. At. Spectrom. 13 (1998) 935–940.
[32] H.P. Longerich, S.J. Jackson, D. Gunther, Laser ablation inductively coupled plasma mass spectrometric transient signal data acquisition and analyte concentration calculation, J. Anal. At. Spectrom. 11 (1996) 899–904.
[33] S. Levitus, T.P. Boyer, World Ocean Atlas, vol. 4, Temperature, 1994, pp. 1–117.
[34] J.I. Martínez, P. DeDeckker, T.T. Barrows, Palaeoceanography of the last glacial maximum in the eastern Indian ocean: planktonic foraminiferal evidence, Palaeogeogr. Palaeoclimatol. Palaeoecol. 147 (1999) 73–99.
[35] J. Erez, A. Almogi-Labin, S. Avraham, On the life history of planktonic foraminifera: lunar reproduction cylce in *Globigerinoides sacculifer* (Brady), Paleoceanography 6 (1991) 295–306.
[36] J.C. Duplessy, P.L. Blank, A.W.H. Be, Oxygen-18 enrichment of planktonic foraminifera due to gametogenic calcification below the euphotic zone, Science 213 (1981) 1247–1250.
[37] L.R. Sautter, Morphologic and stable isotopic variability within the planktic foraminiferal genus *Neogloboquadrina*, J. Foraminifer. Res. 28 (1998) 220–232.
[38] A.W.H. Bé, J.K.B. Bishop, M.S. Sverdlove, W.D. Gardner, Standing stock, vertical distribution and flux of planktonic foraminifera in the Panama Basin, Mar. Micropaleontol. 9 (1985) 307–333.
[39] L.R. Sautter, R.C. Thunell, Seasonal variability in the δ^{18}O and δ^{13}C of planktonic foraminifera from and upwelling environment: sediment trap results from the San Pedro Basin, Southern California Bight, Paleoceanography 6 (1991) 307–334.